DOI: 10.48011/asba.v2i1.1294

An economic D-RTO for thermal solar plant: analysis and simulations based on a feedback linearization control case

Igor M. L. Pataro [*] **Marcus V. Americano da Costa** [**]
Lídia Roca [***] **José L. Guzmán Sanches** [*] **Manuel Berenguel** [*]

[*] *Department of Informatics, University of Almería, Ctra. Sacramento s/n 04120, Almería, Spain*
[**] *Department of Chemical Engineering, Federal University of Bahia, 02 Professor Aristides Novis St., Salvador, BA-40210910, Brazil.*
[***] *CIEMAT-Plataforma Solar de Almería, CIESOL, Ctra. de Senés s/n, Tabernas 04200, Almería, Sapin*

Abstract: This work proposes an economic dynamic real-time optimization (D-RTO) strategy to control a solar collector field in order to maximize the amount of thermal power energy delivered to multi-effect seawater distillation plant. A validated model of the compound parabolic concentrator collector field of the AQUASOL plant, available at the Plataforma Solar de Almería (Spain), is used as case study. The optimization algorithm is based on receding horizon optimization problem, in which an economic function takes into account the energy produced by the solar plant and the electricity consumption costs by the water pump. The D-RTO strategy is compared to a feedback linearization controlling in different temperature setpoints, intending to analyze economic benefits and viability of the proposed algorithm. Simulation results show the D-RTO algorithm is capable of handling process disturbances and operating in economic benefit conditions, bringing good perspectives for implementation in real applications.

Keywords: Dynamic optimization; solar energy; desalination process; feedback linearization control.

1. INTRODUCTION

With the idea of sustainable development, governments and the modern society recognize the use of renewable energy as an alternative to reduce dependence on conventional sources of polluting energy. Changes in the energy model are promoting technological progresses and improving the quality of human life around the world. In this context, solar energy has received a special attention. This source of clean energy is practically inexhaustible and has a high technical potential for use as it reaches the entire planet. In particular, solar thermal generation is projected to be responsible for the production of 12% of all world energy by 2040 (Agency, 2011).

Solar thermal energy has been applied for many purposes such as desalination (Roca et al., 2008), heating and cooling (Americano-daCosta et al., 2014), generation of electricity (Karthick et al., 2019), and distillation (Americano-daCosta and Santos, 2015; Salem et al., 2020). The main concept of the thermal solar process is to use an internal fluid, known as heat transfer fluid (HTF), that circulates through the solar collectors and is heated by the incident irradiance and its thermal transfer. The volumetric flow rate of the heat transfer fluid may be manipulated to control the final temperature at a desired point while compensates the changes in solar irradiance and ambient temperature.

The solar thermal plants can have different configurations depending on the types of collectors, HTF (synthetic oil or water) to produce low (below of 100^oC), or medium (100 to 300^oC), or high (above 300^oC) temperatures (Goswami, 2015). Thus, this type of process deals with different problems known by the automatic control community such as nonlinear dynamics, delay times, variant parameters and many disturbances. In the literature, it is possible to find a great number of studies and applications of control techniques applied on solar thermal plants (Camacho et al., 2012). Traditional PID controllers have been used (Pasamontes et al., 2011), but advanced control strategies have presented better results (Camacho and Gallego, 2015). Also, many works have been dedicated to the development of mathematical models and simulation of solar thermal processes (Americano-daCosta et al., 2020). Although there are important studies focused on achieving optimal operation of solar thermal plants, for instance Gallego et al. (2013); Vega and Cuevas (2018); Gil et al. (2020), there is still motivation to explore dynamic optimization in these processes, especially when economic aspects are considered. In fact, according to industrial experts, the optimization layer can increase a profitability of a process by 7% to 10%. Payback times of six months to a year are often claimed on such projects (Brosilow and Joseph, 2002).

Real-time optimization (RTO) is not an appropriate procedure to solar plants, since its formulation uses a steady-

state model to determine the best operation points and weather conditions disturb this type of process all the time. In this case, Dynamic-RTO (D-RTO) can be used to calculate the optimal setpoints that maximizes the system's profits considering the range constraints and current measured disturbances. Powell et al. (2013) demonstrated the possibility of increasing efficiency in solar thermal plants using dynamic optimization strategy. Nevertheless, the main purpose is the optimal operation by means heat dynamic integration to thermal energy storage and energy demand. For that, models of systems and disturbances are required. An improvement of that work was done, in which a fossil fuel component was included to the system in order to maximize the total solar energy collected over a 24 h period (Powell et al., 2014). Other studies considering economic optimization can be found, but often employed to size and design solar thermal plants that uses standard control techniques or only accounts energy fluxes (Winterscheid et al., 2017).

On the other hand, recently, researchers have concerned to dynamically optimize the operation of solar plants from an economic point of view. Scolan et al. (2020) proposed a dynamic optimization based on load curve (mass flow rate and temperature) of a complex large-scale solar thermal plant with the objective to sell energy as heat. Modelling and validation for individual units such as solar field, heat exchanger, and storage tank were performed to ensure realistic simulations. The results show an increase of 6.2% of the energy provided to the consumer, a redution of 62% of electricity consumption, and economic profit gains by 2.1%.

Thus, based on foregoing, an economic dynamic real-time optimization strategy to control solar thermal processes and maximize its energy production is proposed in this paper. The algorithm considers the disturbance inputs (ambient temperature, irradiance, and inlet solar field temperature) and updates the optimal inlet volumetric flow rate, according to a cost function of accumulated energy and operating constraints that also include the control goals. For the simulations, experimental data and the validated model of the CPC (compound parabolic concentrator) collector field of the AQUASOL plant at the Plataforma Solar de Almería, located in Spain, are used to analyze different scenarios. The results are based on Roca et al. (2008)'s work, in which a feedback linearization control was applied on the plant.

The paper is organized as follows: in Section 2, the AQUASOL system and solar field model are described. In Section 3, the D-RTO formulation is developed and the whole algorithm is explained. In Section 4, the simulations are presented and results are discussed. The conclusions from the study are stated in Section 5.

2. PLANT DESCRIPTION AND MODELLING

The AQUASOL plant at the Plataforma Solar de Almería consists of a CPC solar collector field, a thermal storage system with 24 m^3 of total volume, a multi-effect distillation (MED) plant, a double-effect absorption heat pump (DEAHP), and an auxiliary gas boiler. The AQUASOL can be operated on three modes: (i) solar, in which the required input temperature of the MED is reached using only the solar field in good weather conditions; (ii) fossil, when MED works supplied by the gas boiler coupled to the DEAHP due to low irradiance or during the night; and (iii) hybrid, in which there is a combination between the previous modes avoiding the gas boiler as much as possible. The whole water desalination process is detailed in the researches of Roca et al. (2008) and González et al. (2014).

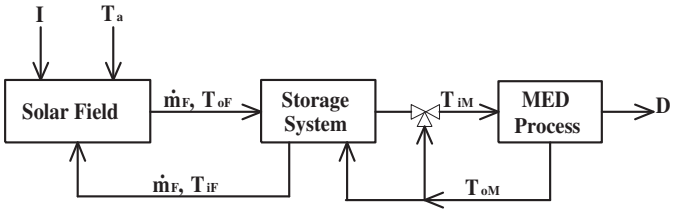

Figure 1. AQUASOL plant on solar mode.

In this work, it is considered the AQUASOL operating on the solar mode, as shown in Figure 1. The water mass flow rate $\dot{m}_F(t)$ (kg/min) with a temperature $T_{iF}(t)$ (^oC) from the storage system pass through the solar field, where it is heated due to thermal changes caused by incident irradiance $I(t)$ (W/m^2) and ambient temperature $T_a(t)$ (^oC). The heated temperature of the water $T_{oF}(t)$ (^oC), produced by the solar field, flows until the tanks where the thermal energy is storaged to feed the MED. The inlet first-effect nominal temperature $T_{iM}(t)$ (^oC) is achieved by mixing water from the storage system and with that one $T_{oM}(t)$ (^oC) returned from the first-effect using a three-way regulation valve. Finally, the fresh water is obtained with a 3 m^3/h nominal distillate production $D(t)$ (m^3).

The solar field is an association of plane collectors in series and parallel, wherein each one has a number of $n_a = 7$ parallel tubes in order to absorb with minimum losses the thermal energy given by the ambient. The system is organized with groups of $n_{cp} = 3$ collectors in parallel, connected to $n_p = 3$ of that in series composing an unit denominated as cell, as is illustrated in Figure 2. Note that the delay time d_c is due to the distance along the pipers between the location of the temperature sensor and the input collector.

Finally, $n_c = 7$ cells in parallel form a solar field row. Thus, $n_l = 4$ rows also in parallel integrate the whole solar field, composed of 252 CPCs with a total surface area of approximately 500 m^2.

This configuration of rows, cells, and collectors can be simplified as a lumped parameter model. The mathematical model used for simulation is based on energy balance of the water which flows into the equivalent absorber tube of length $Leq = L \cdot n_p$, in which L is the CPC tube length, given by Roca et al. (2008):

*Corresponding author. E-mail addresses: ilp428@inlumine.ual.es (I. Pataro), marcus.americano@ufba.br (M.V. Americano da Costa), joseluiz.guzman@ual.es (J. L. Guzmán), beren@ual.es (M. Berenguel). lidia.roca@psa.es (L. Roca)

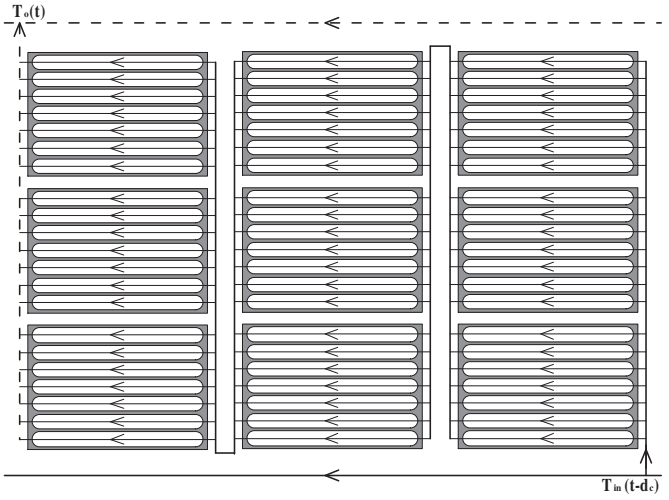

Figure 2. Unit cell composed of 3x3 collectors.

$$\rho \cdot c_p \cdot A_a \cdot \frac{\partial T_{oF}(t)}{\partial t} = \beta \cdot I(t) - \frac{H}{L_{eq}} \cdot (\bar{T}(t) - T_a(t)) - c_p \cdot \dot{m}_{eq}(t) \cdot \frac{(T_{oF}(t) - T_{iF}(t - d_c))}{L_{eq}}, \quad (1)$$

$$\bar{T}(t) = \frac{T_{oF}(t) + T_{iF}(t - d_c)}{2}, \quad (2)$$

wherein the constant parameters are shown in Table 1, and the delay time is modeled as:

$$d_c(t) = \frac{L_d \cdot A_a}{F_f(t)}, \quad (3)$$

and $\dot{m}_{eq}$ is calculated as:

$$\dot{m}_{eq}(t) = \frac{\dot{m}_F(t)}{n_l \cdot n_c \cdot n_{cp} \cdot n_a}, \quad (4)$$

in which $F_f(t)$ (m^3/min) and $\dot{m}_{eq}$ (kg/min) are the volumetric flow rate and mass flow rate of the water, respectively. L_d represents the distance along the tubes between the inlet temperature sensor and the input solar plant, and the measured outlet temperature is given by:

$$T_o(t) = T_{oF}(t - d_o),$$

wherein $d_o = 4/6\ min$ is the fixed output delay time.

Table 1. Process parameters

Name	Value
absorber cross-section area, A_a	$7.85 \cdot 10^{-5}$ m^2
water steam specific thermal capacity, c_p	4190 $J/(kg \cdot^o C)$
thermal losses coefficient, H	4.7 $J/(s \cdot^o C)$
equivalent absorber tube length, L_{eq}	4.5 m
irradiance model parameter, β	0.105 m
water density, ρ	975 kg/m^3
CPC tube length, L	1.89 m
Equivalent tube length, L_{eq}	5.67 m
Equivalent tube flow, $\dot{m}_{eq}$	$\dot{m}_F/588$ kg/min

Thereby, the water temperature is obtained by varying its volume flow rate $F_f(t)$ and taking the energy coming from the solar irradiance. On one hand, given a range of disturbances values (T_{iF}, I, T_a), it is possible to heat the water by reducing its flow rate. On the other hand, increasing the desired outlet temperature T_{oF}, the quantity of accumulated mass water decreases. This is an interesting optimization and control problem that will be seen later.

3. DYNAMIC OPTIMIZATION ALGORITHM

In this work, it is used the method of orthogonal collocation on finite elements, capable of determining optimal control trajectories by given the description of process, the cost function, equality and inequality constraints and the time interval length of optimization. The optimization problem is solved by complete parametrization of control and state profiles vector, approximated by a sequence of linear combination. Since the basis function is already known, the optimization is performed by minimizing the linear combination coefficients, that is, the control and states vectors.

One of the advantages of this algorithm is that the basis function is defined as open-loop ordinary differential equation (ODE) or differential-algebraic equations (DAE) of the process, which are well known for CPC solar collector plants and can be simply implement in computational software, as *Matlab*, for instance. Moreover, since analytical equations are used, the gradients of the control vector and states, as well as the objective function, can be solved by formal calculus, which presents better results when compared to the numerical approximation. Thus, the optimization and control strategy is formulated applying the *DynOpt* algorithm developed by Cižniar et al. (2005) for *Matlab*.

In this case, the process behavior is described in the form $M\dot{x}(t) = f(x(t), u(t))$, wherein the M is known as constant mass matrix. This ODE system equation forms equality constraints for the optimization problem, written as the Mayer form (Cižniar et al., 2005).

3.1 Optimization Problem Design

Considering the system described in Section 2, the main objective of the optimization problem is to provide the production of distilled water from the greater use of renewable energy provided by the production of hot water in the thermal solar field. Thus, the optimization problem considers to maximize the amount of energy produced by the CPC collector field taking into account the outlet temperature T_{oF}, the water mass flow $\dot{m}_{eq}$, and the controlling ranges. It is important to mention that the D-RTO strategy uses the nonlinear dynamic model of the process and model uncertainties can deteriorate its performance with changes in numerical iterations. Therefore, for the purpose of improving the optimizer closed-loop robustness, a low-pass filter $F_r(s) = 1/(T_f s + 1)$ is employed for the output error $e(t) = T_{oF}(t) - T_{oFm}(t)$, in which T_{oFm} is the outlet temperature model. The dynamic optimization and control scheme is shown in Figure 3. Notice that the D-RTO takes into account the disturbances and essential states of the process, calculates an optimal dynamic curve and, thereby, gives a discrete signal $u(kT_s)$ for each T_s sample time.

In order to formulate the optimization problem in the Mayer form, Equations 5 and 6 are proposed, in which the first state is the outlet temperature $x_1(t) = T_{oF}(t)$, described in Equation 1, and the second state is the

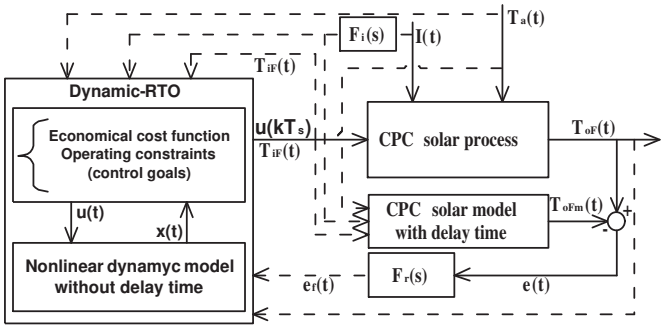

Figure 3. Solar field optimization and control scheme.

economic-objective function $x_2(t) = J_{ec}(t)$, that is minimized by the optimizer. In addition, the input variable is the volumetric flow of water $u(t) = \dot{m}_F/\rho$. Hence, the differential equation is defined as a system of equations $f(x_1, x_2, u, t)$ in which:

$$\dot{x}_1(t) = f_1(x_1, u, t) = \frac{T_{oF}}{dt} \tag{5}$$

$$\dot{x}_2(t) = f_2(x_1, u, t) = \alpha \cdot c_1 \cdot d_v(t) \cdot u(t) \cdot \rho \cdot C_p \cdot (x_1(t) - T_{oF\,min}) - c_2 \cdot E_c(u(t)) \tag{6}$$

wherein α is the weight parameter. $d_v(t) = (1 - e^{(-0.167 \cdot t)})$ is the proposed valve-pump dynamic, although real process behavior may diverge. Equation 6 can be separated in two terms: the right one refers to the cost associated to electricity consumption caused by the solar field pump, in which E_{ec} is calculated in euros, given $c_2 = 1.53 \cdot e^{-6}$ €/W, in the form (González et al., 2014):

$$E_c(u(t)) = 191.4 \cdot u^2(t) - 479.5 \cdot u(t) + 663.8. \tag{7}$$

On the left is calculated the benefits, wherein $c_1 = 8.171 \cdot e^{-10}$ €/J represents the approximated value for each joule required by the MED plant, considering a minimum operating temperature $T_{o_{min}}$ to produce fresh water. The heated water price is estimated by the total distilled water production in simulations performed by González et al. (2014). To simplify implementation, d_v is considered only on benefit term, since it presents a higher magnitude.

Therefore, the optimization problem can be formulated as:

$$\min_{u(t)} \; -x_2(x_1(t), u(t), t) = -\int_0^{h_f} J_{ec}(x_1(t), u(t), t) \cdot dt \tag{8}$$

subject to Equations (5), (6) and:

$$x_1(h_f) = T_{oF}(h_f) \tag{9}$$

$$T_{iF} + \Delta T_{min} + e_f(t) \leq x_1(t) \leq T_{max} + e_f(t) \tag{10}$$

$$\dot{m}_{F_{min}}(t) \leq \rho \cdot u(t) \leq \dot{m}_{F_{max}}(t) \tag{11}$$

being $e_f(t)$ the filtered error between the process and model outputs; ΔT_{min} and T_{max} the outlet temperature limits, and $\dot{m}_{F_{min}}(t)$ and $\dot{m}_{F_{max}}(t)$ the mass flow limits. Note that the D-RTO configuration is a receding horizon optimization problem, wherein the algorithm is solved repeatedly over a moving prediction time horizon h_f. Volumetric flows are calculated to maximize thermal energy produced by the solar field and to minimize the electricity consumption of the pump, according to the control constraints. For the proposed algorithm, the gradients are analytically calculated and considered in the optimization problem as:

$$\frac{\partial f}{\partial x} = \begin{bmatrix} \frac{\partial f_1}{\partial x_1} & \frac{\partial f_2}{\partial x_1} \\ \frac{\partial f_1}{\partial x_2} & \frac{\partial f_2}{\partial x_2} \end{bmatrix}, \; \frac{\partial f}{\partial u} = \begin{bmatrix} \frac{\partial f_1}{\partial u} & \frac{\partial f_2}{\partial u} \end{bmatrix}, \; \frac{\partial f}{\partial t} = \begin{bmatrix} \frac{\partial f_1}{\partial t} & \frac{\partial f_2}{\partial t} \end{bmatrix}.$$

4. RESULTS

In this section, the proposed D-RTO algorithm is simulated in different scenarios aiming to evaluate its economic performance and the perspective of practical applications. A feedback linearization control (FBL) strategy, proposed by Roca et al. (2008), is used only as reference, wherein the non-linear mapping formulation integrated to classical linear controllers (in that case a PI controller with anti-windup) allows solar fields to operate at the limit with great results in economic point of view. In this work, the inlet and outlet temperature delays for the CPC model plant are considered for both the D-RTO and FBL, as well as a low-pass filter in the solar irradiation signal, to attenuate strong variations in the model. In addition, an attenuation factor $a = 0.4$ for β is used only for the FBL control strategy.

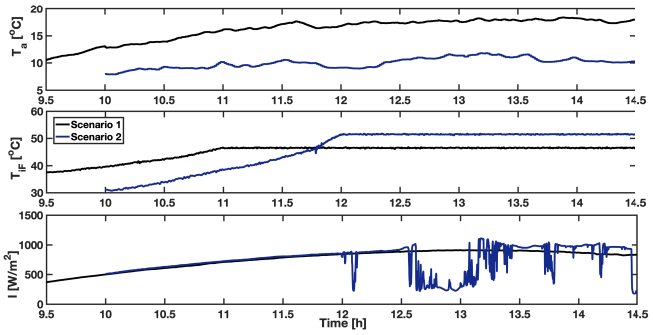

Figure 4. Process disturbances - Scenario 1 and 2.

Figure 4 shows disturbances of Scenarios 1 and 2. For the first scenario, solar irradiance is uniform and presents very slight variations. For the second scenario, stronger variations occur in solar irradiance which can represent a cloudy day. In both cases, the process is regulated to acquire energy above 66.5 ^{o}C, which is considered the minimum temperature to operate the MED unit, and, then, the inlet temperature T_{iF} is maintained constant. The useful energy production of the solar plant is considered only when T_o is greater than $T_{o_{min}} = 62.5$ ^{o}C and less than $T_{max} = 86.5$ ^{o}C, which for this case study is considered the maximum temperature allowed for the plant, regarding safety criteria, even though, the costs of operating the pump are considered throughout the simulation. Moreover, it is considered the solar field pump characteristics, wherein the maximum inlet flow is limited to $28.2 \cdot 10^{-2}$ m^3/min, the minimum flow limited to $6.0 \cdot 10^{-2}$ m^3/min, the sample time $T_s = 1$ and the dynamic behavior $d_v(t)$, as defined in Section 3. For the nominal case, a weigh tuning constant $\alpha = 0.4$ is used to improve performance of D-RTO algorithm and the optimization horizon is set to $h_f = 1$ min.

Since the purpose of this work is to analyze the proposed D-RTO algorithm, it is important to emphasize that these simulated scenarios are defined to provide a broader range of conditions and, thereby, expand the limits to evaluate the performance of the dynamic optimization strategy, although, in real process the difference in inlet and outlet temperature is maintained between 5 ^{o}C and 20 ^{o}C to avoid stress in CPC materials (Roca et al., 2008; González et al., 2014).

To compare the D-RTO performance, FBL control is used for different outlet temperature set-points, in order to scan the best operating point. This control strategy has been applied in real case and has achieved interesting control performance for the CPC plant (Roca et al., 2008). Therefore, the FBL approach is used to reproduce a real operating situation, in which the operator tries to deal with the trade-off between greater energy production and the lowest electricity energy costs by the pump, varying the outlet temperature gradients to achieve optimum economic conditions. Figure 5 shows the CPC outlet temperature and the volumetric water flow for both D-RTO and FBL algorithms simulated in Scenario 1. Notice that the FBL cases follow an initial setpoint for $T_{iF} + 10$ and, latter, for $T_{iF} + 20$ with slight overshoot when changing the ramp. Then, when T_o reaches 66.5 ^{o}C, the setpoints are set to 66.5^{o}C, 70 ^{o}C, 75 ^{o}C, 80 ^{o}C, and 85.0 ^{o}C. It may be seen that the FBL controller keeps the outlet temperature in the desired setpoint for all gradients. However, at 85.0 ^{o}C, the controlled variable overpasses the maximum temperature limit. Regarding the D-RTO algorithm, it is possible to notice that CPC plant operates closest to the maximum limit in relation to the constrains, applying very low water flow since high temperatures improve useful energy production. In addition, D-RTO ensures an optimal input flow curve and fast response from the beginning to reach the minimum temperature to produce useful heated water. It is important to highlight the advantage of the predictive feature in accordance to the energy production considered in the optimization problem formulated in Section 3.

In order to analyze economic performance, Table 2 presents the performance indices for all cases in Figure 5. The profits gains are related to the amount of fresh water produced by the MED unit, from the energy produced from hot water in the CPC plant. Notice that the D-RTO strategy achieves the highest profits of €7.816 with the lowest running costs, in which, in other words, it produces the greatest amount of energy, even though the amount of water at the end of the simulation is the lowest, comparing to other cases. It may also be noticed that the higher the set-point, the greater the amount of energy produced by the FBL, achieving €7.344 for 80.0 ^{o}C set-point. However, due to control variations and disturbances, for 85.0 ^{o}C set-point, the FBL controller case passes 86.5 ^{o}C and this production is not considered, hence, producing only €4.073.

In Scenario 2, wherein there are strongest variations in solar irradiation, Table 3 and Figure 6 show the performance of FBL and D-RTO, however, only the best FBL case is reproduced on graphs. In this scenario, FBL controller is set to follow initial setpoint of $T_{iF} + 20$, and, latter, fixed setpoints identical to Scenario 1. It may be noticed

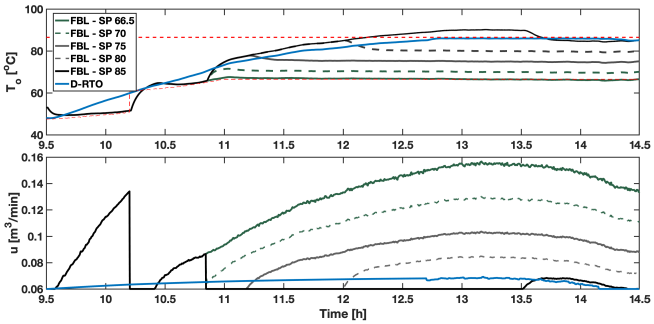

Figure 5. Output temperature and inlet water flow for Scenario 1.

Table 2. Performance indices for D-RTO and FBL cases in Scenario 1.

Scenario	Profit (€)	Hot Water (m^3)	Running costs (€)
D-RTO	7.862	19.04	0.171
FBL/SP=66.5^{o}C	1.719	36.71	0.236
FBL/SP=70.0^{o}C	4.838	31.57	0.197
FBL/SP=75.0^{o}C	6.429	26.42	0.176
FBL/SP=80.0^{o}C	7.344	22.83	0.172
FBL/SP=85.0^{o}C	4.073	20.19	0.175

that the CPC plant loses energy production when strong disturbance occurs, however, the D-RTO continues to respect the constraints when the irradiation level rises again. Thus, it is evident that the control performance reflects on MED profits. The FBL best result achieves €3.920, whereas the D-RTO was capable to produce more energy and, hence, would produce more fresh water, achieving €5.813 of profits. For FBL higher set-points, the control strategy pass the 86.5 ^{o}C limit, not contributing to the total energy production, since if the maximum operating temperature is overpassed in real case it could damage the structure.

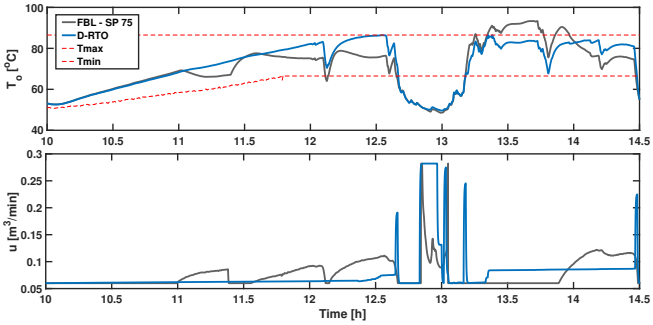

Figure 6. Output temperature and inlet water flow for Scenario 2.

Table 3. Performance indices for D-RTO and FBL cases in Scenario 2.

Scenario	Profit (€)	Hot Water (m^3)	Running costs (€)
D-RTO	5.813	21.04	0.186
FBL/SP=66.5^{o}C	2.797	32.73	0.262
FBL/SP=70.0^{o}C	3.814	26.03	0.185
FBL/SP=75.0^{o}C	3.920	20.91	0.162
FBL/SP=80.0^{o}C	2.893	17.91	0.161
FBL/SP=85.0^{o}C	2.224	17.34	0.158

As can be seen in Scenario 2, the D-RTO shows interesting results for strong disturbance. Thus, aiming to evaluate the optimization algorithm robustness, uncertainties scenarios were also simulated. β and H parameters are chosen to represent the source of model uncertainties. In fact, it encloses all the uncertainties of the terms $\beta/(\rho \cdot c_p \cdot A_a)$ and $H/(\rho \cdot c_p \cdot A_a \cdot L_{eq})$ in Equation 1. Table 4 shows the performance indices for each parameter variations, simulated in Scenario 1. To achieve better results, after several simulated experiments, a first order low-pass filter is used in the irradiation signal, with $T_i = 10$ min. The robust filter is adjusted to $F_r(s) = 1/(50s + 1)$ and the weight constant to $\alpha = 0.075$, which, in practical analyses, minimizes more the electricity energy costs in the optimization problem than the previous scenarios. The performance indices show that the D-RTO algorithm presents good performance for uncertainties cases, for both β and H parameters, approximating its behavior to the nominal case. Nevertheless, since the model plant is more sensitive to the β parameter, the performance is more deteriorated, but it still operates in economical benefits, achieving 66.2% of profits of the nominal case for the worst case. Therefore, these results bring us a good perspective of practical applications, even thought robustness studies must be done to ensure profits in cases with higher errors.

Table 4. Performance indices for β and H uncertainties in Scenario 1

Scenario	Profit (€)	Hot Water (m^3)	Running costs (€)
+10% $\times\beta$	7.815	19.83	0.170
+10% $\times H$	7.206	22.55	0.169
+20% $\times\beta$	7.209	22.80	0.201
+20% $\times H$	6.874	23.83	0.170
-10% $\times\beta$	6.692	24.49	0.172
-10% $\times H$	7.826	19.73	0.170
-20% $\times\beta$	5.191	29.25	0.191
-20% $\times H$	7.825	19.78	0.170

5. CONCLUSIONS

A D-RTO optimization algorithm is proposed for a CPC solar plant, operating as energy supply source to a MED distillation facility. The D-RTO structure is based on a one-layer receding horizon optimization problem, in which the economic function takes into account the amount of energy produced by the CPC plant and the costs associated to the electricity consumption by the water pump. The optimization algorithm is compared to a validated FBL control strategy method for different temperature gradients.

The results shows that the D-RTO is capable of maximizing the amount of energy produced by the CPC, or, in other words, the thermal power supplied, even with strong disturbances. Moreover, the preliminary results show that the D-RTO optimization problem can maximize economic conditions whit no necessity to define an specific reference for the controlled variables, only by correctly designing the process limits as problem constraints. This results brings good perspectives since it facilitates the CPC plant operation in maximum power, which, in fact, represents a MED operation as stable and profitable as possible and a more efficient use of solar energy. Furthermore, the D-RTO algorithm shows robustness accomplishment by adding a robust filter in the predicted output, improving performance on mismatch cases.

Finally, the optimization algorithm has good expectation for implementation in real scenario. Future work regarding robustness analysis could be carried out. In addition, a more in-depth analysis with predictive control and optimization strategies is intended.

ACKNOWLEDGMENT

The authors would like to thank National Council for Scientific and Technological Development - CNPq - Brazil (PhD Program Abroad/ Process n^o 201143/2019-4) for financial support and CIEMAT for providing data of the AQUASOL plant at the Plataforma Solar de Almería - Spain.

REFERENCES

Agency, I.E. (2011). *Solar Energy Perspectives*. Organisation for Economic Co-operation and Development/IEA, Paris, France.

Americano-daCosta, M.V. and Santos, T.L.M. (2015). Using solar irradiation for steam generation in bioethanol production: An initial study. In *6th International Renewable Energy Congress (IREC)*, 1–6.

Americano-daCosta, M.V., Narasimhan, A., Guillen, D., Joseph, B., and Goswami, D.Y. (2020). Generalized distributed state space model of a CSP plant for simulation and control applications: Single-phase flow validation. *Renewable Energy*, 153, 36 – 48.

Americano-daCosta, M.V., Pasamontes, M., Normey-Rico, J.E., Guzmán, J.L., and Berenguel, M. (2014). Advanced control strategy combined with solar cooling for improving ethanol production in fermentation units. *Ind. Eng. Chem. Res.*, 53(28), 11384–11392.

Brosilow, C. and Joseph, B. (2002). *Techniques of Model-based Control*. Prentice-Hall, New Jersey.

Camacho, E.F. and Gallego, A.J. (2015). Model predictive control in solar trough plants: A review. *IFAC-PapersOnLine*, 48(23), 278 – 285. 5th IFAC Conference on Nonlinear Model Predictive Control NMPC 2015.

Camacho, E.F., Soria, M.B., Rubio, F.R., and Martínez, D. (2012). *Control of Solar Energy Systems*. Advances in Industrial Control. Springer-Verlag London.

Cižniar, M., Salhi, D., Fikar, M., and Latifi, A. (2005). A matlab package for orthogonal collocations on finite elements in dynamic optimisation. *15th Int. Conference Process Control 2005*. Strbské Pleso, Slovakia.

Gallego, A., Fele, F., Camacho, E., and Yebra, L. (2013). Observer-based model predictive control of a parabolic-trough field. *Solar Energy*, 97, 426 – 435.

Gil, J.D., Roca, L., Zaragoza, G., Normey-Rico, J.E., and Berenguel, M. (2020). Hierarchical control for the start-up procedure of solar thermal fields with direct storage. *Control Engineering Practice*, 95, 104254.

González, R., Roca, L., and Rodríguez, F. (2014). Economic optimal control applied to a solar seawater desalination plant. *Computers & Chemical Engineering*, 71, 554 – 562.

Goswami, D.Y. (2015). *Principles of Solar Engineering*. Taylor & Francis, third edition.

Karthick, K., Suresh, S., Hussain, M.M.M., Ali, H.M., and Kumar, C.S. (2019). Evaluation of solar thermal system configurations for thermoelectric generator applications: A critical review. *Solar Energy*, 188, 111 – 142.

Pasamontes, M., Álvarez, J.D., Guzmán, J.L., Lemos, J.M., and Berenguel, M. (2011). A switching control strategy applied to a solar collector field. *Control Engineering Practice*, 19(2), 135 – 145.

Powell, K.M., Hedengren, J.D., and Edgar, T.F. (2013). Dynamic optimization of a solar thermal energy storage system over a 24 hour period using weather forecasts. In *2013 American Control Conference*, 2946–2951.

Powell, K.M., Hedengren, J.D., and Edgar, T.F. (2014). Dynamic optimization of a hybrid solar thermal and fossil fuel system. *Solar Energy*, 108, 210 – 218.

Roca, L., Berenguel, M., Yebra, L., and Alarcón-Padilla, D.C. (2008). Solar field control for desalination plants. *Solar Energy*, 82(9), 772 – 786.

Salem, M.R., Salem, M.R., Higazy, M., and Abdrabbo, M. (2020). Performance enhancement of a solar still distillation unit: A field investigation. *Solar Energy*, 202, 326 – 341.

Scolan, S., Serra, S., Sochard, S., Delmas, P., and Reneaume, J.M. (2020). Dynamic optimization of the operation of a solar thermal plant. *Solar Energy*, 198, 643 – 657.

Vega, J. and Cuevas, C. (2018). Simulation study of a combined solar and heat pump system for heating and domestic hot water in a medium rise residential building at concepción in chile. *Applied Thermal Engineering*, 141, 565 – 578.

Winterscheid, C., Holler, S., and Dalenbäck, J.O. (2017). Integration of solar thermal systems into existing district heating systems. *Energy Procedia*, 116, 158 – 169. 15th International Symposium on District Heating and Cooling, September 2016, Seoul, South Korea.